PHYSICAL REVIEW B **78**, 180506(R) (2008)

Valence-band and core-level photoemission spectroscopy of $LaFeAsO_{1-x}F_x$

A. Koitzsch,[1] D. Inosov,[1] J. Fink,[1,2] M. Knupfer,[1] H. Eschrig,[1] S. V. Borisenko,[1] G. Behr,[1] A. Köhler,[1] J. Werner,[1] B. Büchner,[1] R. Follath,[2] and H. A. Dürr[2]

[1]*Institute for Solid State Research, IFW Dresden, P.O. Box 270116, D-01171 Dresden, Germany*

[2]*BESSY GmbH, Albert-Einstein-Strasse 15, 12489 Berlin, Germany*

(Received 7 August 2008; revised manuscript received 16 September 2008; published 20 November 2008)

We have investigated the electronic structure of $LaFeAsO_{1-x}F_x$ ($x=0;0.1;0.2$) by angle-integrated photoemission spectroscopy and local-density approximation (LDA)-based band-structure calculations. The valence band consists of a low-energy peak at $E\approx-0.25$ eV and a broad structure around $E\approx-5$ eV, which are in qualitative agreement with LDA. From the photon-energy dependence of these peaks we conclude that the former derives almost exclusively from Fe 3*d* states. This constitutes experimental evidence for the strong iron character of the relevant states in a broad window around E_F and confirms theoretical predictions.

DOI: 10.1103/PhysRevB.78.180506 PACS number(s): 74.70.Dd, 71.20.Be

The recent discovery of the superconducting oxypnictides has sparked immediate and intense scientific effort. Naturally the question about the origin of superconductivity is the driving force of the field, especially since the same problem for the cuprate high-temperature superconductors still awaits solution. Here superconductivity is found in yet another tetragonal highly two-dimensional system. Therefore the materials offer a fresh perspective on the general problem of high T_c and, possibly, insight into (so far) elusive aspects.

Superconducting transition temperatures up to $T_c=43$ K have been reached for $LaFeAsO_{1-x}F_x$.[1,2] Substitution of La by other rare-earth elements enhances T_c even further to values beyond 50 K.[3,4] As in the cuprate superconductors and in some heavy fermion compounds, superconductivity is found in proximity to magnetic ordering. For undoped LaOFeAs a commensurate antiferromagnetic phase is found below 140 K.[5,6] Several studies present experimental evidence for *s*-wave pairing[9,10] but the existence of line nodes cannot be excluded at present.[7,8,11] The electronic structure and its implications for superconductivity have been investigated from the theoretical side in Refs. 12–17. $LaFeAsO_{1-x}F_x$ crystals consist of alternating $LaO_{1-x}F_x$ and FeAs layers. It is assumed that the $LaO_{1-x}F_x$ layers serve as ionic charge reservoirs for the covalently bound metallic FeAs layers where the superconductivity appears. According to band-structure calculations the layered crystal structure translates into a highly two-dimensional electronic structure with cylindrical Fermi-surface sheets. The density of states (DOS) in the vicinity of the Fermi energy is dominated by iron character. Previous photoemission studies found gross agreement between experiment and theory.[9,18,19]

Here we report on angle-integrated photoemission measurements of $LaFeAsO_{1-x}F_x$ ($x=0,0.1,0.2$). We have measured the photointensity of polycrystalline material for various excitation energies ranging from $h\nu=15$ to 200 eV at $T=30$ K. Experimentally a peak near the Fermi energy and a second broad structure of several electron volts below E_F are observed for all doping levels. From the excitation-energy dependence we conclude that the near-E_F peak consists predominantly of iron states. We find doping-dependent quantities in the valence and core-level spectra. The energy position of the lines shifts generally to higher energies with electron doping.

Polycrystalline samples of $LaFeAsO_{1-x}F_x$ were prepared by using a two-step solid-state reaction method similar to that described by Zhu *et al.*[20] The samples consist of $1-100$ μm sized grains of $LaFeAsO_{1-x}F_x$. The crystal structure and the composition were investigated by powder x-ray diffraction (XRD) and wavelength dispersive x-ray spectroscopy (WDX). Critical temperatures of $T_c\approx23$ K and $T_c\approx10$ K for $x=0.1$ and 0.2, respectively, have been extracted from magnetization and resistivity measurements. The undoped sample shows a transition to a commensurate spin-density wave below $T_N=138$ K.[6] The XRD analysis shows a phase purity of 96%, 92%, and 89% for $x=0$, 0.1, and 0.2, respectively.

The data were measured using synchrotron radiation at the 1^3 ARPES (angle-resolved photoemission spectroscopy) station with a Scienta R4000 spectrometer at BESSY. The energy resolution was better than 25 meV for excitation energies below 100 eV and better than 40 meV for excitation energies up to 200 eV. The measurements have been performed at temperatures below 30 K. The samples have been scraped *in situ* before measurements at a pressure of $p=1\times10^{-7}$ mbar. The base pressure in the measurement chamber was $p=1\times10^{-10}$ mbar.

Figure 1 presents the valence band of undoped LaOFeAs taken with different photon energies. For reasons explained below the spectra have been normalized to the high-energy shoulder of the broad peak centered at about $E\approx-5$ eV (marked by the arrow). We compare the experimental data to LDA-based orbital resolved DOS calculations in panel (b). The main features of the valence band for all photon energies are the peak near the Fermi energy at $E\approx-0.25$ eV and the broad peak around $E\approx-5$ eV.[22] Note that the peak near E_F is not cut off by the Fermi edge step. The inset of panel (a) shows a zoom of the vicinity of E_F for $h\nu=15$ eV. The Fermi edge appears as a small slope change at the low-energy tail of the spectral weight near E_F, which is clearly visible at low temperatures only. In between the near-E_F peak and the broad peak, a plateaulike region is observed with a small peak at $E\approx1.7$ eV. The broad peak has a complex structure and consists at least of two separate features. The low-energy peak and the broad peak have a significant dependence on the photon energy. The intensity of the low-energy peak increases drastically with increasing photon en-

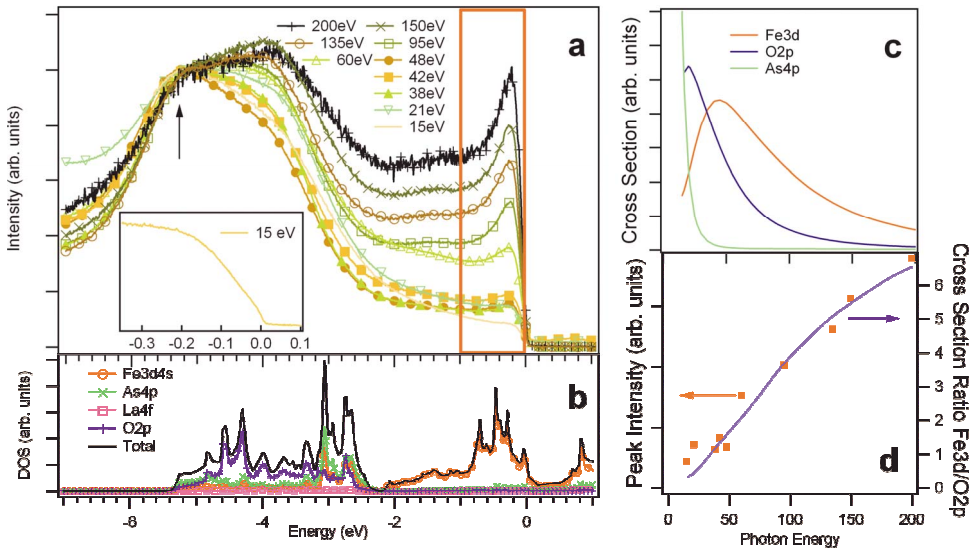

FIG. 1. (Color online) (a) $h\nu$-dependent photoemission valence-band spectra of LaOFeAs. The arrow marks the point of normalization. The red rectangle is the integration window for the low-energy weight shown in panel (d); the inset shows the near E_F region for $h\nu=15$ eV. Note the small change at $E=0$ which indicates the Fermi edge. (b) Local-density approximation (LDA)-derived orbital resolved DOS (density of states). (c) Atomic photoemission cross section for the relevant orbitals (Ref. 21). (d) Ratio of the Fe $3d$ and O $2p$ cross sections from (c) (line) compared to experimental values obtained by integrating the low-energy peak (squares).

ergy relative to the broad peak. The center of gravity of the broad peak shifts toward lower energies due to the intensity increase in the low-energy shoulder, which becomes more intense than the high-energy shoulder at $h\nu=95$ eV. The presented spectra are taken at $T=30$ K, but no major changes are observed when crossing the magnetic ordering temperature of $T_N=138$ K.

The reason for the $h\nu$-dependent intensity variations lies in the $h\nu$ dependence of the photoemission cross section. The opposite behavior of the high-energy shoulder of the broad peak and the low-energy peak suggests that they arise from different atomic orbitals. We show the energy dependence of the cross section of the potentially important valence orbitals, namely, Fe $3d$, As $4p$, and O $2p$, as a function of photon energy in Fig. 1(c). As $4p$ is important for low energies (<25 eV) only. For energies above ~ 25 eV the spectra will be governed by Fe $3d$ and O $2p$ emissions. For increasing photon energy Fe $3d$ dominates. Figure 1(d) shows the ratio of the cross sections Fe $3d$/O $2p$ (blue line). It increases monotonically in the measured range and reaches a value of 6.5 for $h\nu=200$ eV. Motivated by the increase in the low-energy peak and the decrease in the high-energy shoulder with increasing $h\nu$, we assume that the former is due to Fe $3d$ and the latter is mainly due to O $2p$. We evaluate the intensity of the low-energy peak by taking the integral from 0 to $E=-1$ eV without any background treatment (red box). Since we normalized the spectra to the high-energy shoulder this integral value corresponds automatically to the experimental intensity ratio. Those values are plotted in Fig. 1(d) as red points. We find satisfactory agreement and conclude *a posteriori* the correctness of our assumptions.

The LDA calculations are in qualitative agreement with these findings. The O $2p$ orbital DOS is found at the high-energy side of the broad structure; the low-energy peak is due to Fe $3d$ and is offset from the Fermi energy. Also there is substantial Fe $3d$ weight in the low-energy side of the broad peak that is in agreement with the increasing intensity with increasing photon energy. The small peak at $E=-1.7$ eV and the plateau can be associated with a small peak in the DOS at the same energy. However, there are also significant discrepancies: compared to theory the energy position of the broad peak is shifted to higher energies. Also, the width of the low-energy peak is smaller in experiment than in theory. According to theory at low photon energies the As $4p$ states should play a more prominent role which is not obvious in the data. Although in Fig. 1 only data for undoped LaOFeAs are shown, we would like to point out that at all doping levels a similar behavior is observed.

In Fig. 2 we investigate the doping dependence of the valence band. Electron doping is achieved by substituting oxygen by fluor atoms in the LaO layers. The LaO layers are considered as chemically inert charge reservoirs. The doping level x corresponds, in this picture, to the number of electrons injected to the FeAs layers per formula unit. We show the doping dependence of the valence band for four different excitation energies in Figs. 2(a)–2(d). The spectra are, in each case, normalized to the number of available electrons in the given energy window weighted by their cross section.[23] We have confirmed that normalization to the La $4d$ or the La $5p$ lines gives qualitatively equivalent results. All doping levels show the same structure of the valence band for all excitation energies: the low-energy peak is followed by a plateau of nearly constant intensity and eventually an intensity increase due to the broad peak feature. For $h\nu=200$ eV [panel (a)] an increase in the plateau intensity is observed with electron doping. For $h\nu=150$ eV excitation energy the results [panel (b)] are similar to $h\nu=200$ eV. Within the studied doping range, the valence band does not dramatically change but preserves its overall structure. The inset of panel (c) shows a comparison of the low-energy peak

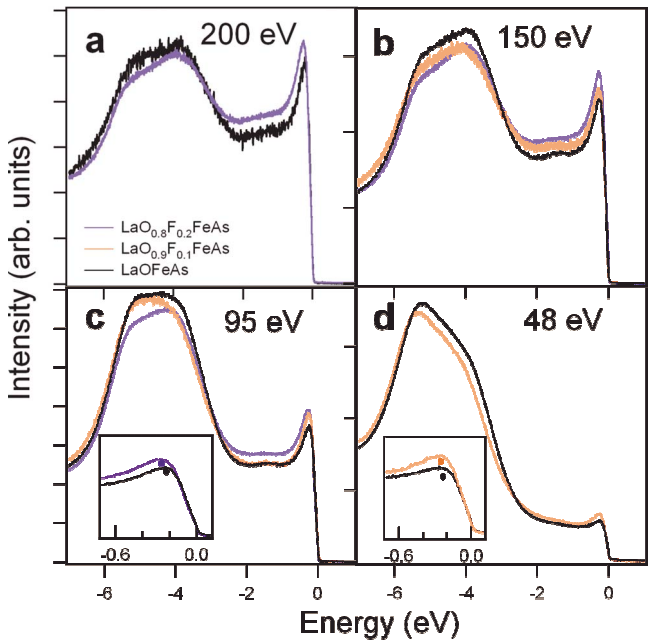

FIG. 2. (Color online) Doping dependence of the valence band for (a) $h\nu$=200, (b) 150, (c) 95, and (d) 48 eV. The spectra have been normalized to their electron count weighted by the photoemission cross section (see Ref. 23). Insets show expanded views on the low-energy region.

for x=0.2 and x=0 F doping. The other doping level has been skipped for clarity. We find a small shift of the peak for electron doping toward higher energies of $\Delta E \approx 30$ meV. The same trend is found for $h\nu$=48 eV [inset of panel (d)] and for the other photon energies. Additionally we find a shift of the broad peak toward larger energies for electron doping.

To investigate possible line shifts in more detail we present the spin-orbit split La 4d and As 3d core levels in Fig. 3 that are measured for different doping levels. The vertical bars indicate the measured peak positions. The peak shifts shown in the inset are referenced to zero doping and refer to the $d_{5/2}$ components at the lower-energy side. The data show a consistent shift toward higher energies for electron doping. The magnitude of the shift is smaller for the As line. The shape of the peaks changes slightly with doping. This seems particularly true for the high binding-energy side and is possibly reflected in the $d_{3/2}$ intensity variations. With doping the chemical environment of La sites is altered in the lattice, therefore, some changes are expected.

The peak shifts indicate a changing chemical potential with doping. Within a rigid-band model electron doping would fill so-far unoccupied states, thereby shifting the chemical potential "to the right." This effectively increases the binding energy of all electronic states. This is the observed effect: the energy increases with electron doping. However, the change in the binding energy of a specific core level depends not only on the chemical-potential shift but also on its chemical surrounding, a possible change in the valence of the atom and screening terms.[24] Having this in mind it is not surprising that the La level shifts more than the As level. The ionic $LaO_{1-x}F_x$ layers are not influenced by valence changes or screening. Additional electrons in the FeAs layers, however, tend to counteract shifts toward higher binding energies. Therefore the observed core-level shift of the La 4d line of ΔE=200 meV for x=0.2 reveals the change in the chemical potential with doping. This interpretation is consistent with our observations for the valence band: the low-energy feature, which consists of iron states, shows only a small shift. The oxygen emission, on the other hand, shows again a clear shift with doping, which is best visible for the $h\nu$=48 eV spectra.

Our experimental observations show that the oxypnictides behave rather like conventional metals than strongly correlated ones: the density of states and the orbital character agree qualitatively with LDA calculations, and the energy

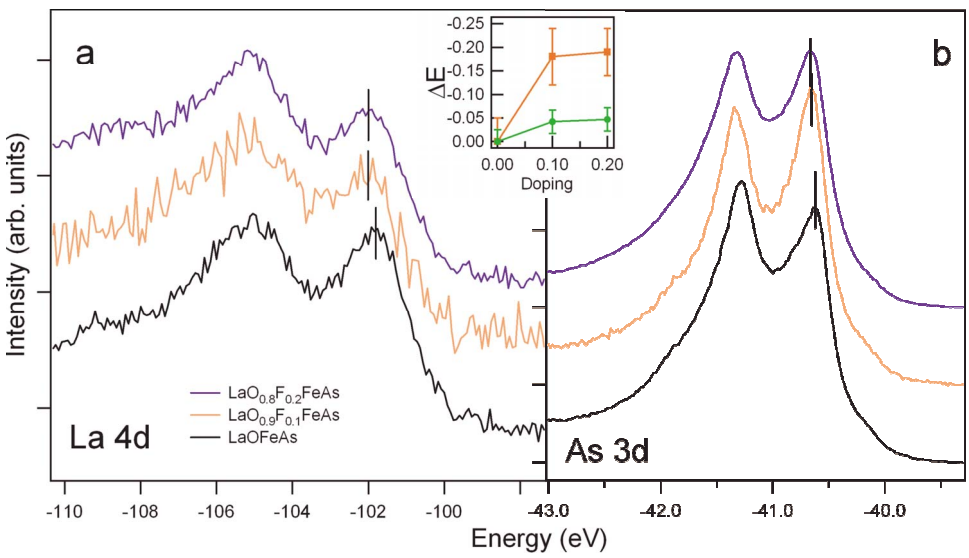

FIG. 3. (Color online) Doping-dependent spectra of $LaFeAsO_{1-x}F_x$ with x=0;0.1;0.2 for (a) La 4d and (b) As 3d. The core levels have been normalized to their integrated intensity. The bars mark the position of the peak maxima. The inset shows the observed peak shifts for La $4d_{5/2}$ (red squares) and As $3d_{5/2}$ (green circles). The spectra are offset vertically for clarity.

shift of the levels follows band filling arguments. This suggests that correlation effects do not play a dominant role for these materials which clearly distinguishes them from the cuprates. Nevertheless they might not be fully negligible due to the observed band narrowing (Fig. 1). Although both materials (cuprates and oxypnictides) have a layered structure with the transition-metal ion on a tetragonal lattice, we find pure iron states at E_F in the oxypnictides instead of strongly hybridized transition-metal ion—ligand states as in the cuprates.

In summary we have investigated the electronic structure of $LaFeAsO_{1-x}F_x$ by angle-integrated photoemission spectroscopy and LDA-based band-structure calculations. From the comparison of the valence band with the theoretical density of states, we find qualitative agreement. From the photon-energy dependence of the spectral weight we explicitly confirm that the low-energy density of states consists predominantly of Fe $3d$ states. We measured the As $3d$ and La $4d$ core levels and find a shift of the chemical potential with electron doping of $\Delta E \approx 200$ meV for $x=0.2$. The entirety of our results suggests that the oxypnictides are not in a strongly correlated regime.

We acknowledge technical assistance by R. Schönfelder and R. Hübel and financial support from the DFG (Grant No. SFB 463).

[1] Y. Kamihara, T. Watanabe, M. Hirano, and H. Hosono, J. Am. Chem. Soc. **130**, 3296 (2008).
[2] H. Takahashi, K. Igawa, K. Arii, Y. Kamihara, M. Hirano, and H. Hosono, Nature (London) **453**, 376 (2008).
[3] Z.-A. Ren, W. Lu, J. Yang, W. Yi, X.-L. Shen, Z.-C. Li, G.-C. Che, X.-L. Dong, L.-L. Sun, F. Zhou, and Z.-X. Zhao, Chin. Phys. Lett. **25**, 2215 (2008).
[4] G. F. Chen, Z. Li, D. Wu, J. Dong, G. Li, W. Z. Hu, P. Zheng, J. L. Luo, and N. L. Wang, Chin. Phys. Lett. **25**, 2235 (2008).
[5] J. Dong, H. J. Zhang, G. Xu, Z. Li, G. Li, W. Z. Hu, D. Wu, G. F. Chen, X. Dai, J. L. Luo, Z. Fang, and N. L. Wang, Europhys. Lett. **83**, 27006 (2008).
[6] H.-H. Klauss, H. Luetkens, R. Klingeler, C. Hess, F. J. Litterst, M. Kraken, M. M. Korshunov, I. Eremin, S.-L. Drechsler, R. Khasanov, A. Amato, J. Hamann-Borrero, N. Leps, A. Kondrat, G. Behr, J. Werner, and B. Büchner, Phys. Rev. Lett. **101**, 077005 (2008).
[7] H. Ding, P. Richard, K. Nakayama, K. Sugawara, T. Arakane, Y. Sekiba, A. Takayama, S. Souma, T. Sato, T. Takahashi, Z. Wang, X. Dai, Z. Fang, G. F. Chen, J. L. Luo, and N. L. Wang, Europhys. Lett. **83**, 47001 (2008).
[8] L. Zhao, H. Liu, W. Zhang, J. Meng, X. Jia, G. Liu, X. Dong, G. F. Chen, J. L. Luo, N. L. Wang, G. Wang, Y. Zhou, Y. Zhu, X. Wang, Z. Zhao, Z. Xu, C. Chen, and X. J. Zhou, arXiv:0807.0398 (unpublished).
[9] L. Shan, Y. Wang, X. Zhu, G. Mu, L. Fang, C. Ren, and H.-H. Wen, Europhys. Lett. **83**, 57004 (2008).
[10] G. Mu, Xiyu Zhu, L. Fang, L. Shan, C. Ren, and H.-H. Wen, Chin. Phys. Lett. **25**, 2221 (2008).
[11] H.-J. Grafe, D. Paar, G. Lang, N. J. Curro, G. Behr, J. Werner, J. Hamann-Borrero, C. Hess, N. Leps, R. Klingeler, and B. Büchner, Phys. Rev. Lett. **101**, 047003 (2008).
[12] L. Boeri, O. V. Dolgov, and A. A. Golubov, Phys. Rev. Lett. **101**, 026403 (2008).
[13] I. I. Mazin, D. J. Singh, M. D. Johannes, and M. H. Du, Phys. Rev. Lett. **101**, 057003 (2008).
[14] D. J. Singh and M.-H. Du, Phys. Rev. Lett. **100**, 237003 (2008).
[15] H. Eschrig, arXiv:0804.0186 (unpublished).
[16] F. Ma and Z.-Y. Lu, Phys. Rev. B **78**, 033111 (2008).
[17] S. Ishibashi, K. Terakura, and H. Hosono, J. Phys. Soc. Jpn. **77**, 053709 (2008).
[18] H. W. Ou, J. F. Zhao, Y. Zhang, D. W. Shen, B. Zhou, L. X. Yang, C. He, F. Chen, M. Xu, T. Wu, X. H. Chen, Y. Chen, and D. L. Feng, Chin. Phys. Lett. **25**, 2225 (2008).
[19] C. Liu, T. Kondo, M. E. Tillman, R. Gordon, G. D. Samolyuk, Y. Lee, C. Martin, J. L. McChesney, S. Bud'ko, M. A. Tanatar, E. Rotenberg, P. C. Canfield, R. Prozorov, B. N. Harmon, and A. Kaminski, arXiv:0806.2147 (unpublished).
[20] X. Zhu, H. Yang, L. Fang, G. Mu, and H.-H. Wen, Supercond. Sci. Technol. **21**, 105001 (2008).
[21] J. J. Yeh and I. Lindau, At. Data Nucl. Data Tables **32**, 1 (1985).
[22] The same spectral shape is found for $h\nu=8$ eV (not shown) indicating no dramatic differences between bulk and surface.
[23] For $x=0$ there are nominally 6 electrons from O $2p$, 6 from Fe $3d$ and 6 from As $4p$, whereas for $x=0.1$ there are only 5.4 for O $2p$, 6.1 from Fe $3d$ and 6 from As $4p$. (The F $2p$ electrons do not count here, because they appear at higher energies.) Those numbers have to be multiplied with their emission probability for the given photon energy and summed up. Here, this type of normalization is close to a normalization to the integrated intensity.
[24] S. Hüfner, *Photoelectron Spectroscopy* (Springer, New York, 1996).